JOINT INSTITUTE FOR NUCLEAR RESEARCH

Veksler and Baldin laboratory of High Energy Physics

FINAL REPORT ON THE SUMMER STUDENT PROGRAM

The study of properties of the thin-gap resistive plate chamber

Supervisors:
Vadim Babkin,
Alexander Dmitriev,
Mikhail Rumiantsev,
V. M. Golovatyuk

Student:
Dmitri Pyrkin (National Research Nuclear University MEPhI), Russia

Participation period:
July 01 – July 31

Dubna, 2016

Abstract

The study of behavior the thin-gap resistive plate chamber (RPC) in various conditions is interesting that it gives better understanding how increase efficiency of multi-gap resistive plate chamber which be used in time-of-flight (TOF) system of the Multi-Purpose Detector (MPD). The uniqueness of this study lies in the fact that so far not investigated detectors with a gas gap of less than 1 mm.

This report shows relations between some characteristics of the RPC such as efficiency, time resolution, voltage amplitude and gap magnitude. During the work it was interesting to see how the operation of the thin-gap RPC detector depends on the gap width and high-voltage. With this knowing we can always calculate or to simulate the detector with any number of gaps.

1 Introduction

1.1 The MPD

The MPD is one of two detectors of international mega-science project "NICA Complex" which aimed at studying the properties of matter in the region of maximum baryonic density formed by heavy ions collisions at $\sqrt{S_{NN}} = 11\ GeV$. In these impacts planned opening of the effects associated with deconfinement phase transition and chiral symmetry restoration. The MPD machine has been designed as a 4π spectrometer capable of detecting of charged hadrons, electrons and photons. To reach this objective, the detector will include accurate 3D-tracking system and high-energy particle identification (PID) system based on the time-of-flight measurements and calorimetry. Despite the difficult physical problem, the basic design requires reasonable budget investments. So it was necessary to use cheap materials in engineering of internal detector systems. The general view of the MPD apparatus is shown in Fig. 1.1.
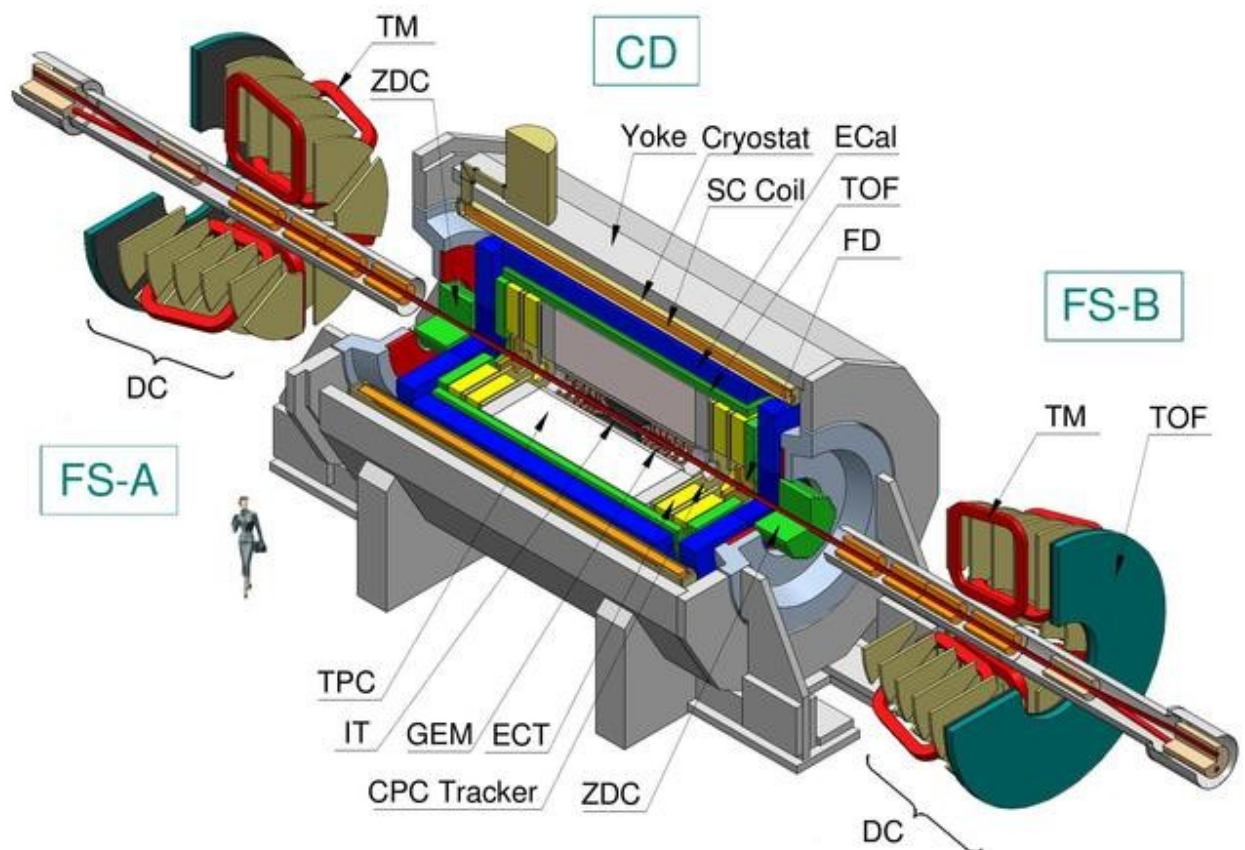
Fig. 1.1. A general layout of the MPD detector.

The detector consist of a lot of subsystems such as: superconductor solenoid (SC Coil) and magnet yoke, inner detector (IT), straw-tube tracker (ECT), time-projection chamber (TPC), time-of-flight system (TOF), electromagnetic calorimeter (EMC), fast forward detectors (FFD), and zero

degree calorimeter (ZDC). Thereby providing cover in particle pseudorapidity region of $|\eta| < 2$.

1.2 Particles identification in the MPD

The ion beams interact inside the beam pipe located along the z-axis with the central interaction point at z = 0 in the centre of the detector. The interaction region covers an interval of $|z| \leq 25$ cm. Ambitious physical problem requires very precision particles identification over as large as possible phase space volume and, consequently, definitions of momentum, energy loss (dE/dx), tracks, time of flight.

The first principal tracker is the time projection chamber (TPC) supplemented by the inner tracker (IT) surrounding the interaction region. Both subdetectors (IT and TPC) have to provide precise track finding, momentum determination, vertex reconstruction and pattern recognition. The second principal tracker is high performance time-of-flight (TOF) detector. With TPC tracking data and fast forward detector (FFD) start signal the TOF system allows to identify charge of hadrons and nuclear clusters. These measurements must be able to know masses as a most common characteristic of all particles complex.

1.3 The TOF system

The basic requirements for the TOF system are:
-       large phase space coverage;
-       high granularity to keep the overall system occupancy below 15%;
-       good position resolution to provide effective matching of the TOF hits with the TPC tracks;
-       high geometrical efficiency (better than 95%);
-       separation of pions and kaons with up to $p_t < 1.5$ GeV/c;
-       separation of (anti)protons with up to $p_t < 3$ GeV/c;
-       TOF detector elements must function in a 0.5 T magnetic field.

At the relatively high momenta of particles the errors in the time of flight measurement and track length definition have higher weight than the error of the momentum determination. The momentum spectra of secondary particles at the NICA colliding energies produced in the regions of pseudorapidity $|\eta| < 1.2$ and $1.2 < |\eta| < 2$ for minimum (4 GeV) and maximum (11 GeV) colliding energies are presented in the Fig. 1.5. The average momentum of pions for energy 4 GeV is about 300 MeV/c and for 11 GeV is about 400 MeV/c.
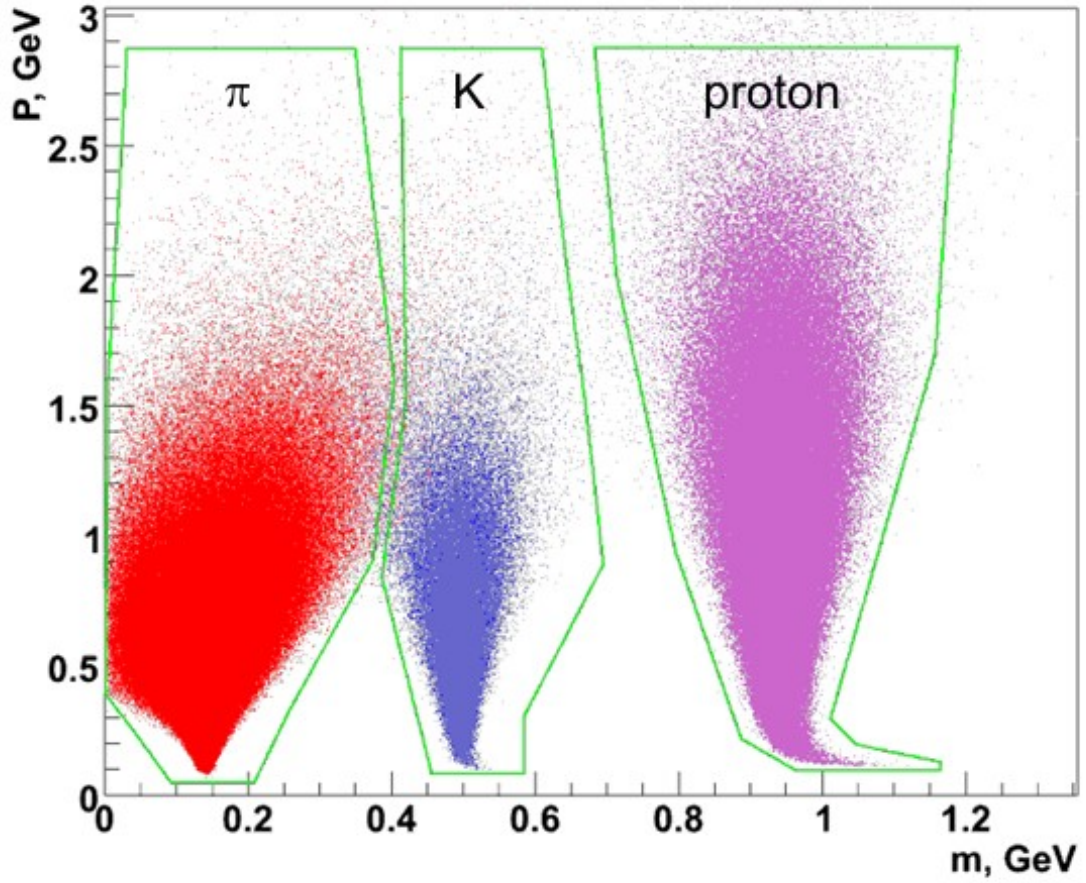
Fig. 2. Mass separation with TOF
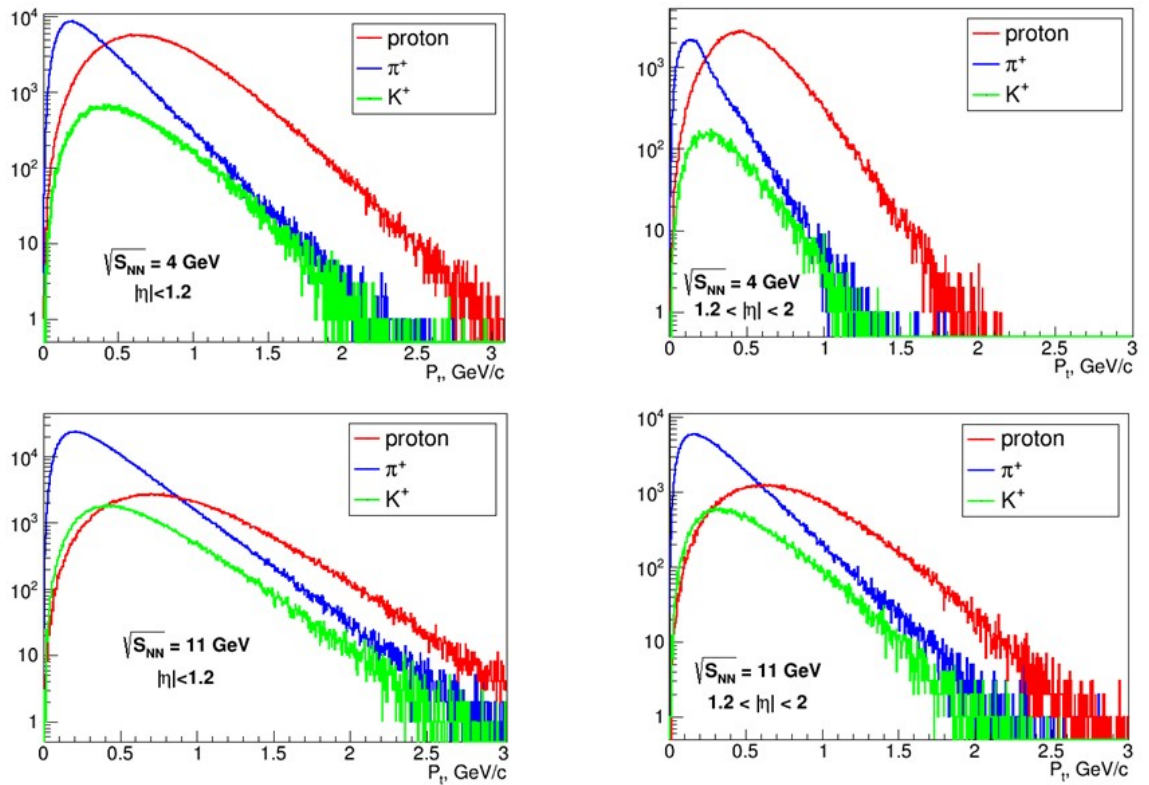
Fig. 3. Momentum spectra of pions, kaons and protons in two regions of pseudorapidity: $|\eta| <$ 1.2 (left) and $1.2 < |\eta| < 2$ (right) and for two center of mass energy: 4 GeV (top) and 11 GeV (bottom)

The smallest track length for the time of flight measurement at the MPD is 1.5 m. We expect to have overall time resolution better than 100 ps. It allows us reliable separation of pions, kaons and protons in the entire interval of momenta for produced particles for the NICA energies.

1.4 The MRPC

Considering these demands and many years of experience in project such as ALICE, PHENIX, STAR, HADES, it was decided to use the multi-gap resistive plate chamber for the TOF system. This type of gaseous detectors combines at the same time good resolution timing, easily manufacturing, relative cheapness and assembling from commercial available materials.

There are two types of MRPC: with the strip signal readout and the pad signal readout. Both PCB options have useful unique features, but in case when multiplicity of events is low, it is preferable to use strips electrode because of the smaller number of channels involved. The example how these two PCB types can looks like are shown in the fig. 1.4.1 and fig. 1.4.2.
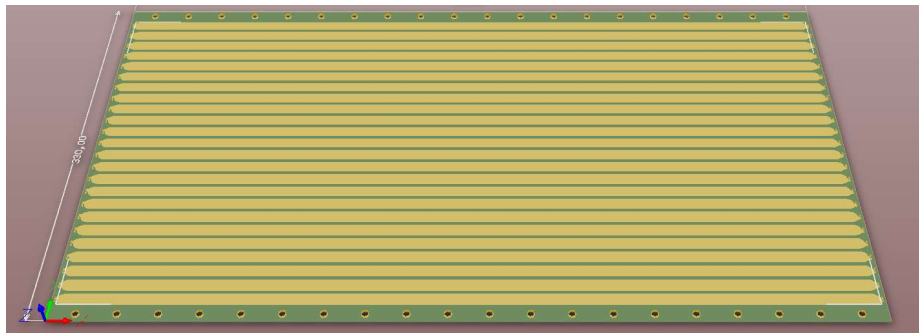
Figure 1.4.1. PCB board with 10 mm wide strips.
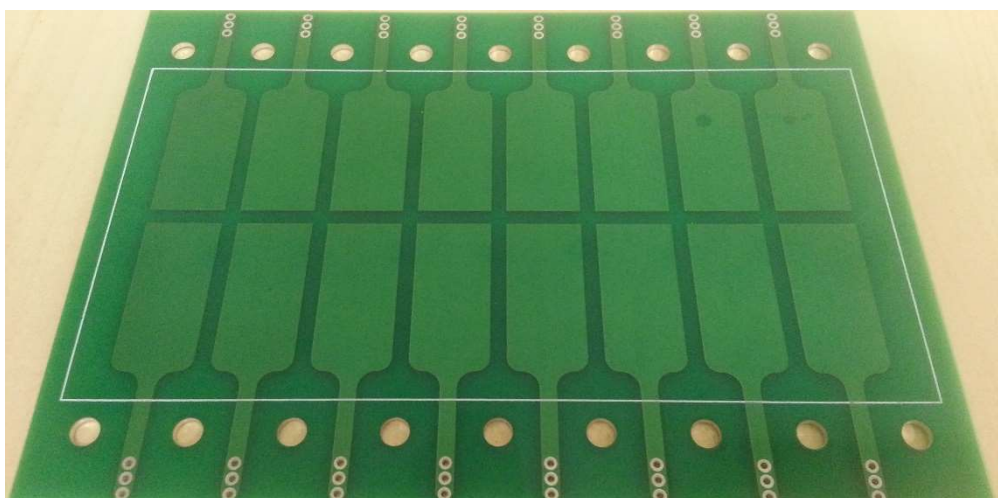
Figure 1.4.2. PCB board with pads.

As we said before the MRPC has simple manufacturing technology. The main idea is that we must create a few small gaseous gaps between two electrodes. The resulting composition called a "stack". For better performance, the creation of detector was proposed on the basis of several such stacks with alternating direction of electric field. Scheme of triple-stack MRPC is shown in fig. 4.
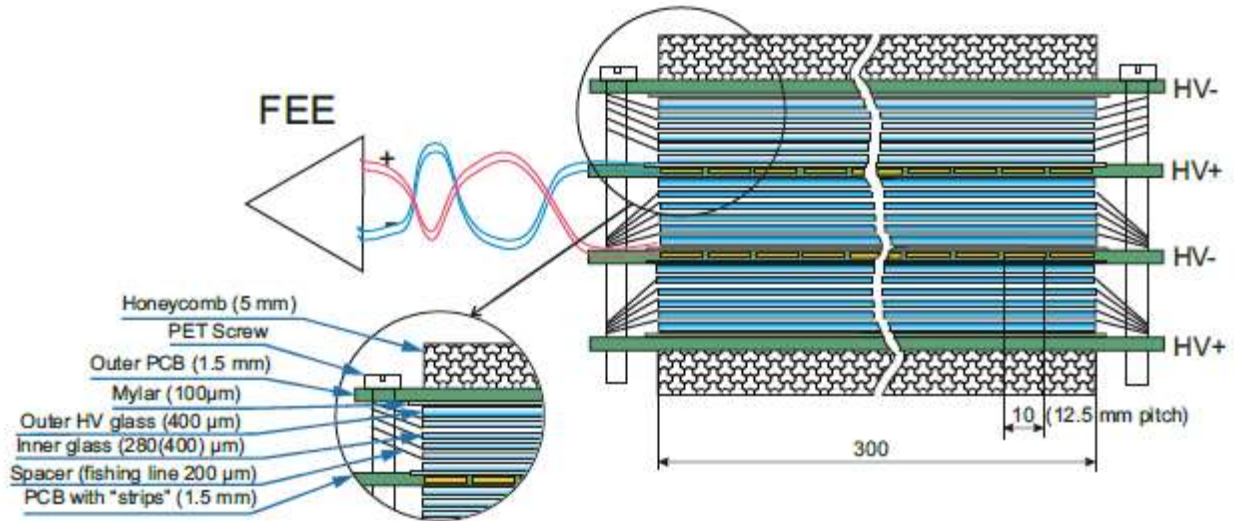
Fig. 4. Scheme of the MRPC.

A more detailed description is given in the next chapter on example of SRPC because of its simplified structure.

2 The thin-gap resistive plate chamber

2.1 The thin-gap RPC structure

The thin-gap RPC consist of two parallel printed circuit boards (PCB) with metallic electrode pads, which needs for readout signals. Positively-charged anode and a negatively-charged cathode made of a glass with graphite conductive layer with surface resistance of $2 - 10$ MΩ per square. Glasses separated from PCB by a layer of mylar insulator. This allows for electrodes placement is sufficiently close to the readout pads. Then fishing line is laid to create a certain gas gap between the electrodes. In our experiment it was decided to exploit two resistive plate chambers with 155 μm and 175 μm gaps. It was made a few steps for rigidity and stability detector: aramid fiber honeycomb panel with a thickness of 5 mm were glued on the external sides of PCBs, PCB boards were tighten by screws, 155μm and 175μm detectors were isolated from each other interference via

the copper foil. Some phases of construction assembling are shown in fig. 2.1.1, 2.1.2, 2.1.3, 2.1.4, 2.1.5, 2.1.6.
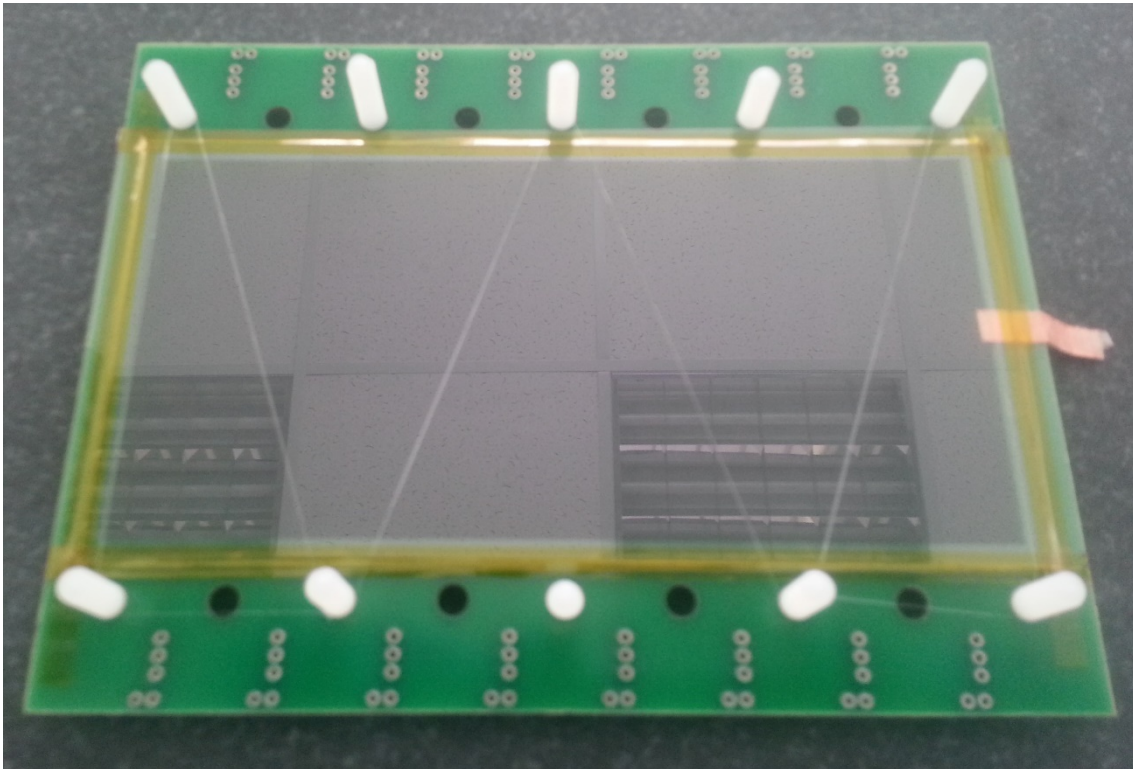
Fig. 2.1.1. Appearance of electrode.
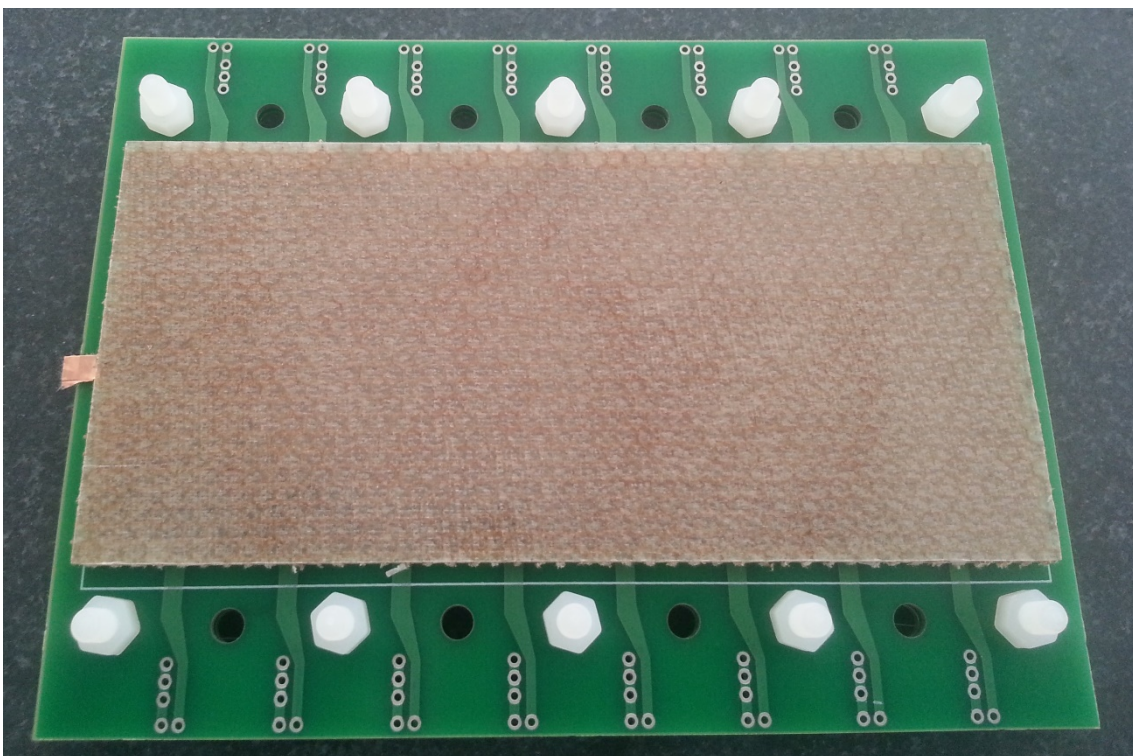
Fig. 2.1.2. A twisting of the PCBs.
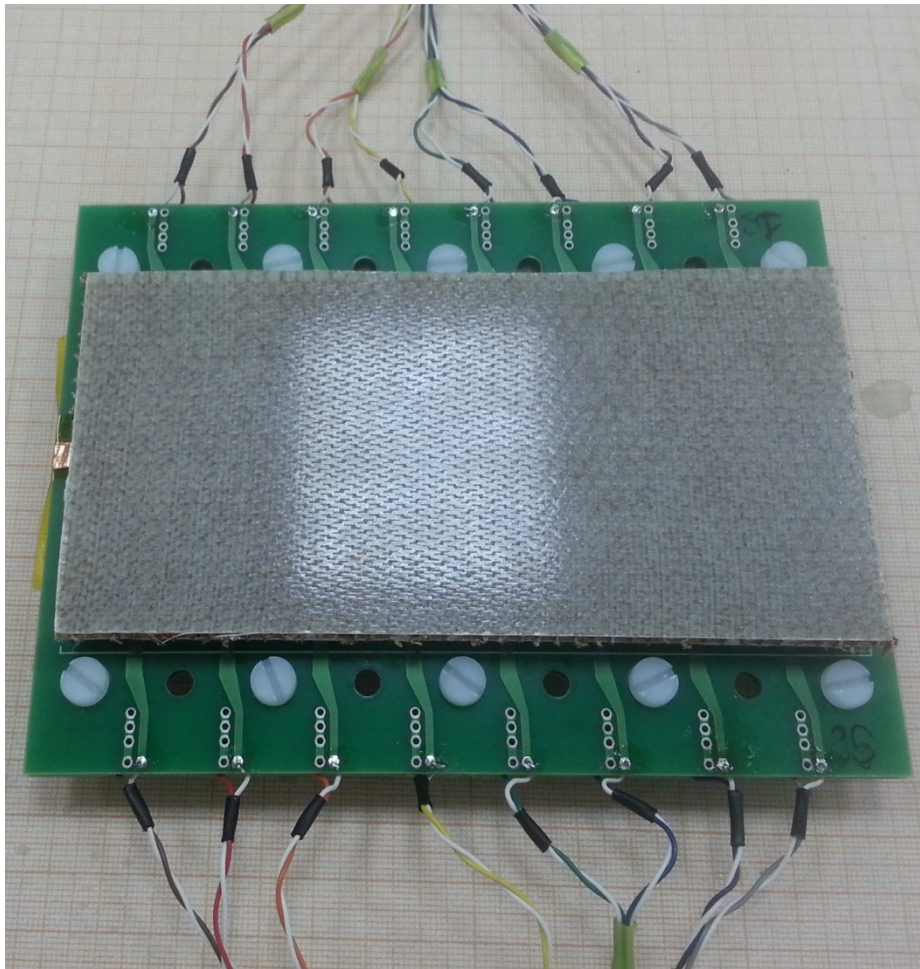
Fig. 2.1.3. Soldered signal cables.
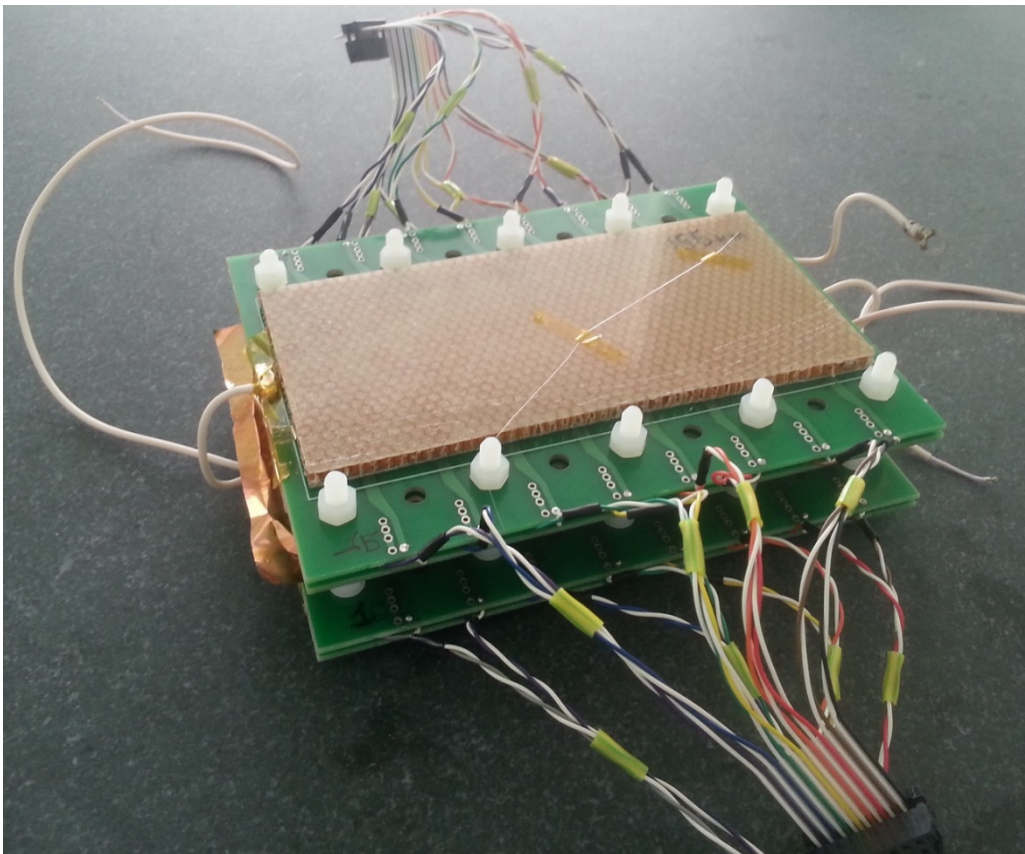
Fig. 2.1.4. Assembly of 155µm (upper) and 175µm (lower) detectors.
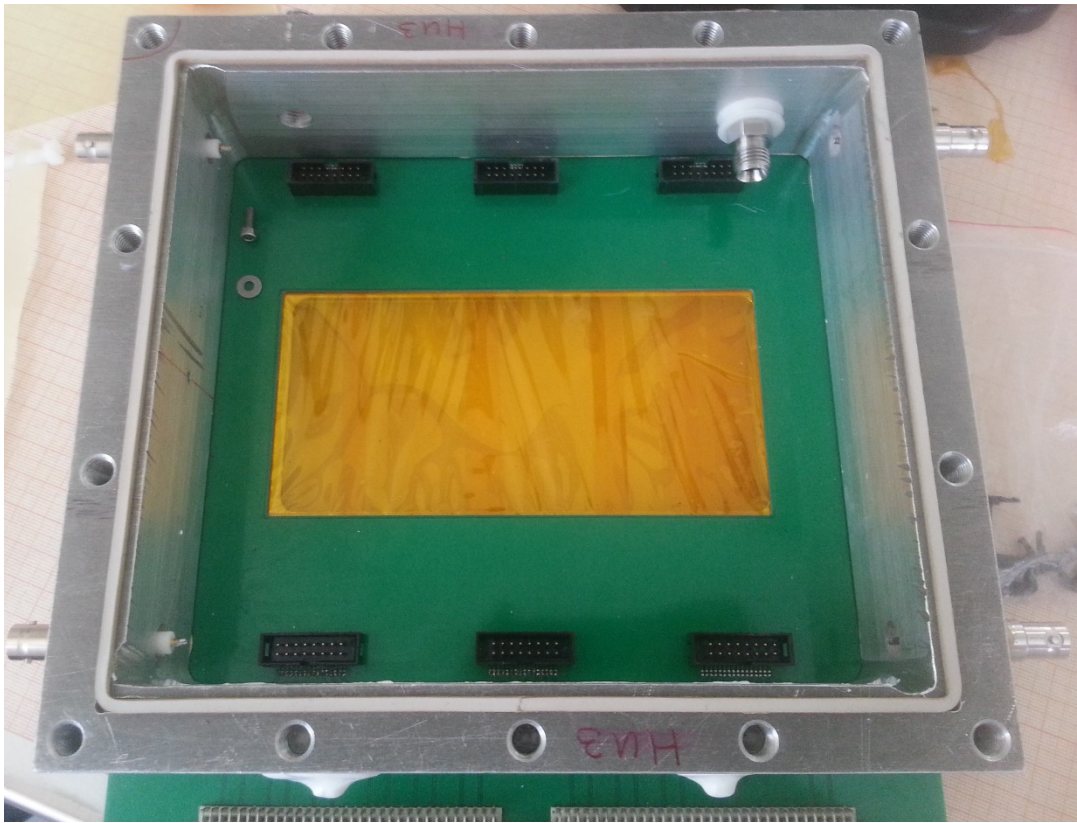
Fig. 2.1.5. A metal box.
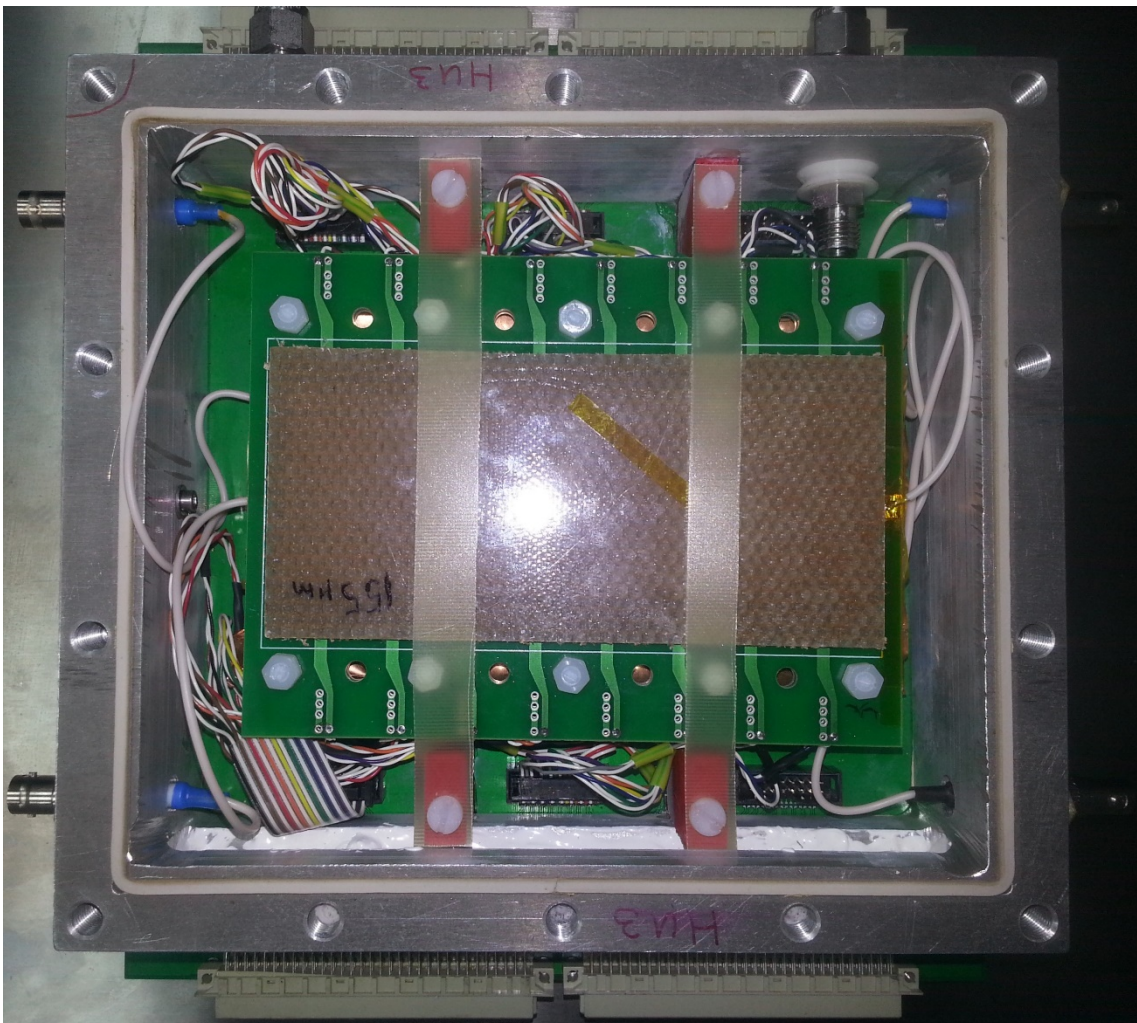
Fig. 2.1.6. A top view of the detector assembly.

2.2 The principles of thin-gap RPC performance

When a particles passes through the chamber, electrons are knocked out of gas atoms. Under electrical field influence, these electrons in turn hit other atoms causing an avalanche of electrons. The electrodes are transparent to the signal (the electrons), which are instead picked up by external metallic pads after a small but precise time delay. Induced signal charge is approximately an order of magnitude less than that generated in gas gap.

At sufficiently high gain, accelerated electrons with enough energy ionized and exited more and more gas molecules. In the result, a small electron avalanches are formed, which can lead to the appearance of streamers. There are two kinds of streamers: anode-directed and cathode-directed. The anode-directed streamer can be presented in the form of droplets, where front parts are light electrons and heavy ions in the tail. Their appearance is not very desirable since their signal is able to completely cover a signal from the particles flights and thus the detector area turn off from a working condition for some time. To combat the streamers box detector filled with a gas mixture, neutralizing the excess number of electrons and photons that excite the local electron avalanches. It is usually used a composition of 90% tetrafluoroethane ($C_2H_2F_4$), 5% isobutene ($i - C_4H_{10}$) and 5% sulfur-hexafluoride (SF_6). But the experiment was conducted in 100% tetrafluorethane for reasons of environmental safety as well as the rest of the impurities are toxic.

In the fig. 2.2. is shown performance scheme of thin-gap resistive plate chamber.
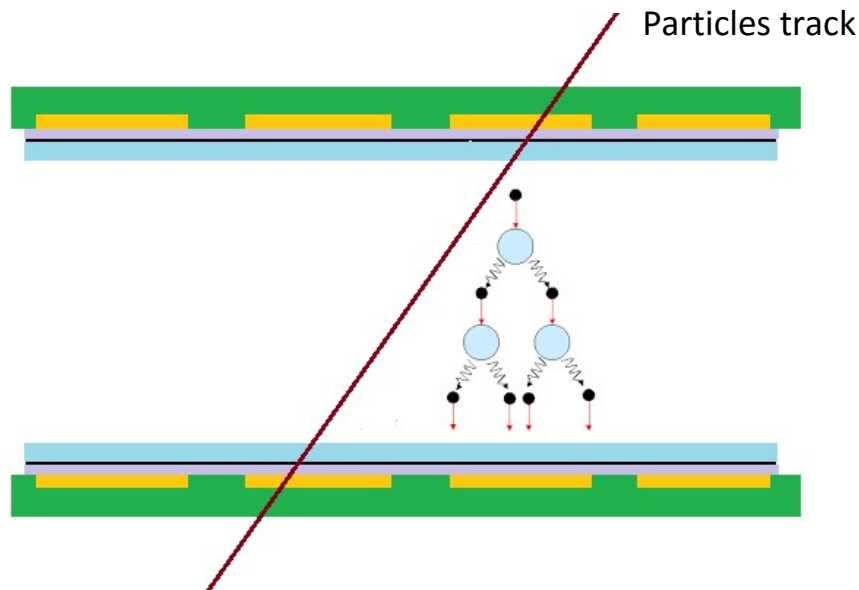
Fig. 2.2. Performance scheme of thin-gap resistive plate chamber.

3 The study of some properties of thin-gap RPC

3.1 The trigger system

The trigger system based on scintillation counters was used for the selection of cosmic particles that pass through the detector. Scheme of this system is shown in fig. 3.2.1 and fig. 3.2.2. It consists of four large scintillators size of 30x15 cm^2 each of which is read from two sides by the two photomultipliers. The small additional counter size of 4x5 cm^2 which included to reduce the solid angle, placed directly above the detectors pads. The signal that is generated by the coincidence of signals from all nine PMTs S1-S8 + S9 is used as start to run the read signals from the detectors.

The distance between the counters S1-4 and S5-8 is equal to 52 cm, S9 counter is 33,5 cm above S5-8. This geometry allows for a solid angle equal to 0.579 sr.
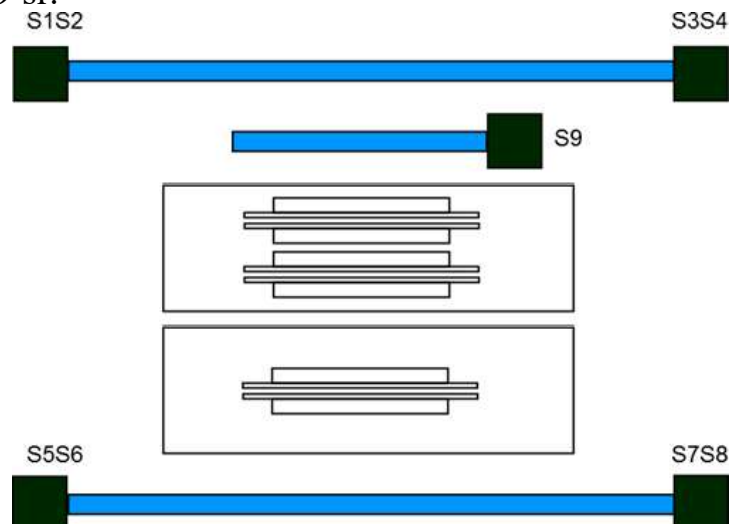
Fig. 3.1.1. Scheme of trigger facility.

Fig. 3.1.2. Isometric view of trigger facility.

3.2 Test setup description

The test was performed in cosmic rays. In this study, we included doublel-stack MRPC with 10 gaps. This type of detector is used in the ALICE experiment in CERN. Due to the large number of gas gap, 10 gaps MRPC is more efficiency then thin-gap RPC. Therefore, we will use it as a valid source of the particle's flight confirmation, in other words - as a reference detector.

Two boxes, one of which comprises two detectors (155µm and 175µm), and other comprises 10 gap MRPC, sequentially connected to 4-channel gas system with MKS-Instruments controllers. Boxes filled with tetrafluoroethane ($C_2H_2F_4$) at atmospheric pressure for increase primary ionization and as a result for better performance.

RPCs were connected to one channel differential analog preamps own design. The analog amplifier is powered by ±5V, input type – differential 55 Ohms, It has a bandwidth of 500 MHz. The amplifier consists of three stages:
• OPA-653 to match the output of the camera;
• AD4960 differential amplifier;
• ADA4937 differential repeater to match the cable.

As the output of a differential pair is used. The total gain is equal to 13.4. The schematic circuit diagram shown in fig. 3.2.

Fig. 3.2. Scheme of analog amplifier.

All signals were read by the digital oscilloscope LeCroy Wave Runner 640Zi with a bandwidth of 4 GHz and 20 Gs/s. Appearance of research setup is shown in fig. 3.2.

Two thin-gap RPCs were under high voltage (HV) of 2000 V.
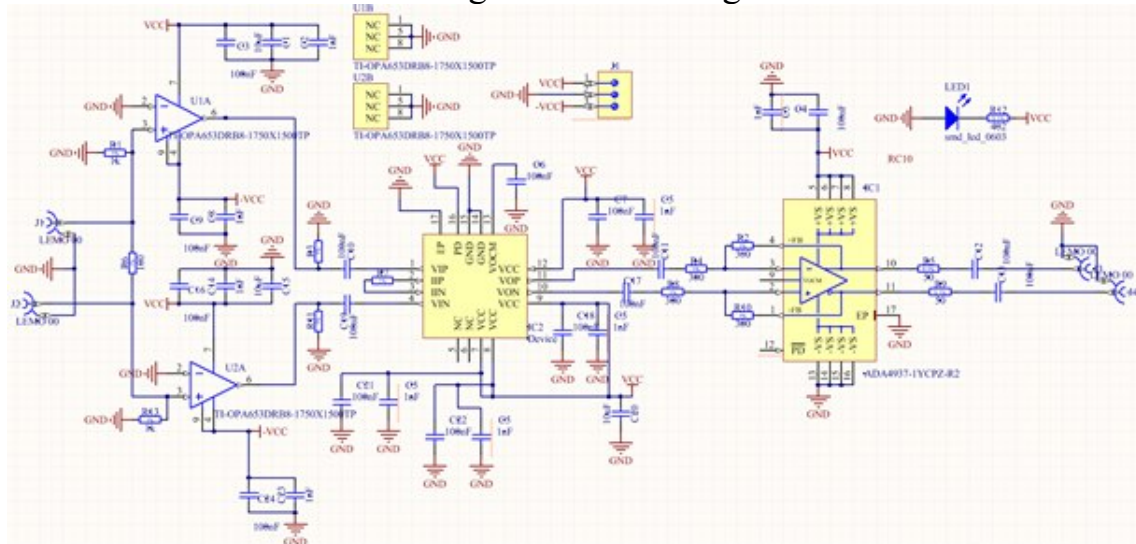
Fig. 3.2. Appearance of cosmic test setup.

4 Results and interpretation

4.1 Signal examples

In this cosmic test, we believe that 10 gaps MRPC is full effective. On figures 4.1.1, 4.1.2 we see the moment of signal coincidences from 175µm and MRPC. The peaks correspond to particles flights, and the rest is noise. The opposite direction of the signal is the result of the using differential amplifier.
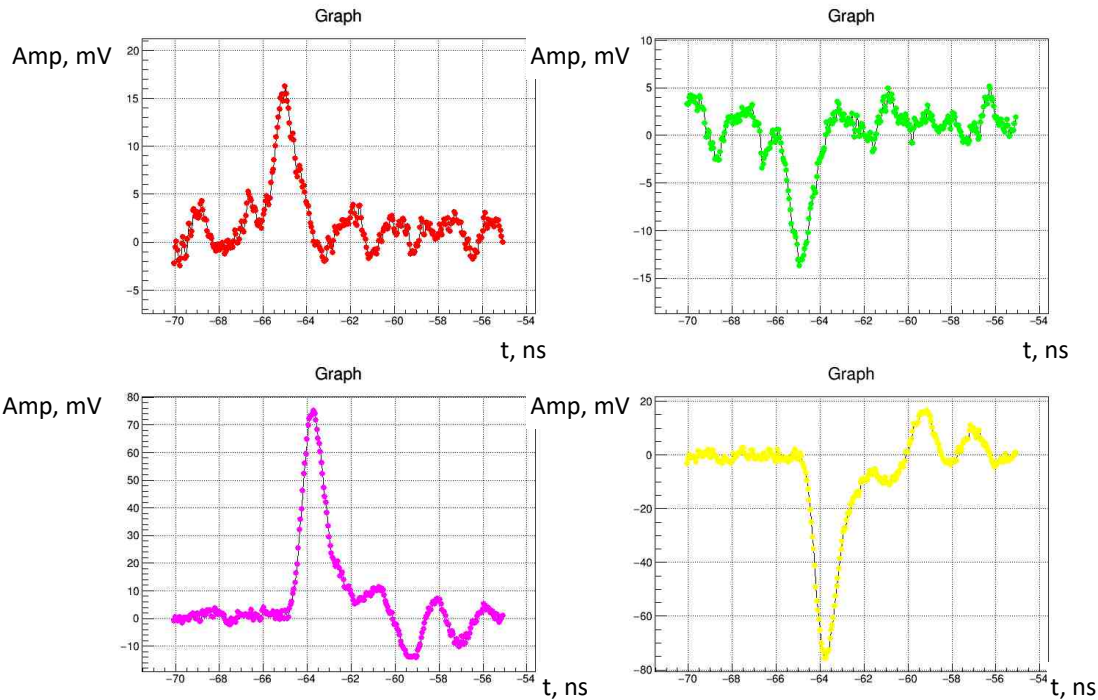
Fig. 4.1.1. Signals from 175µm (upper) and 10 gaps MRPC (lower).
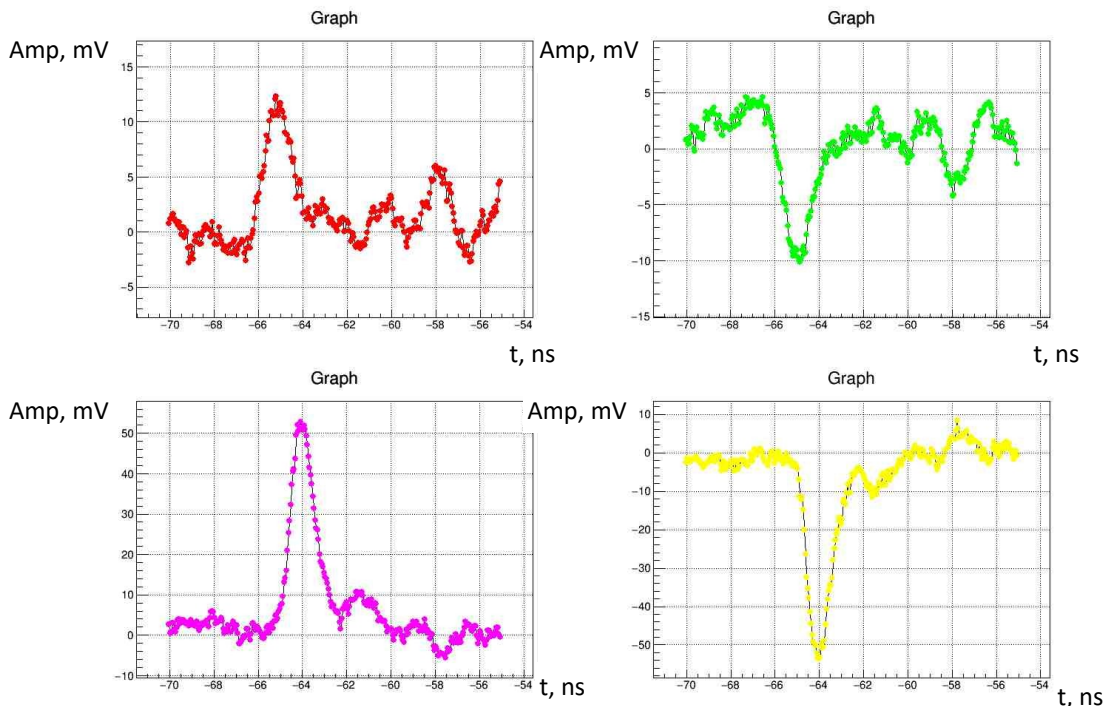
Fig. 4.1.2. Signals from 175µm (upper) and 10 gaps MRPC (lower).

4.2 Noises spectra

It was required to separate useful signals from noises signals for making amplitude histograms. Therefore, we obtained the noise histogramms which are shown in fig. 4.2.1 and 4.2.2.
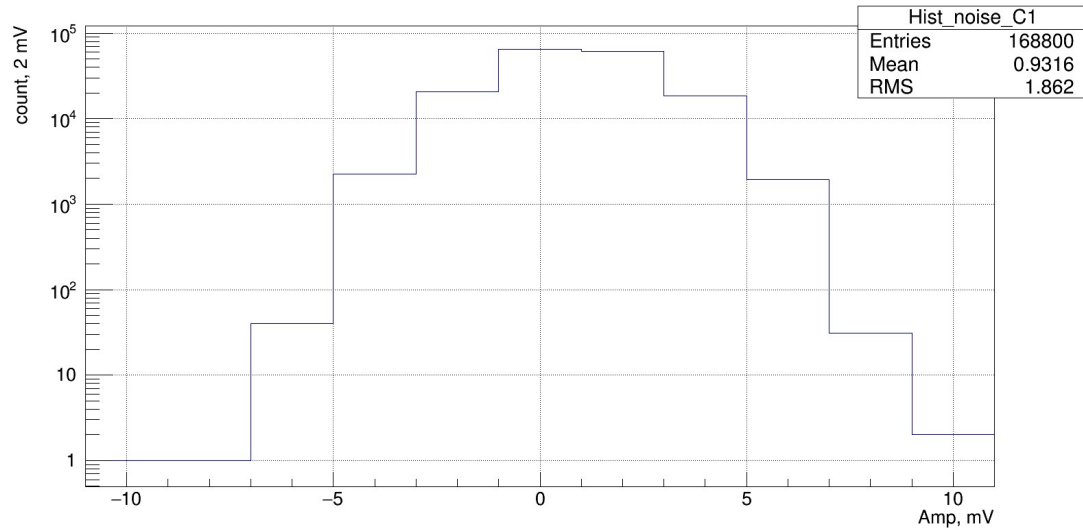
Fig. 4.2.1. Noise of 175 µm RPC.
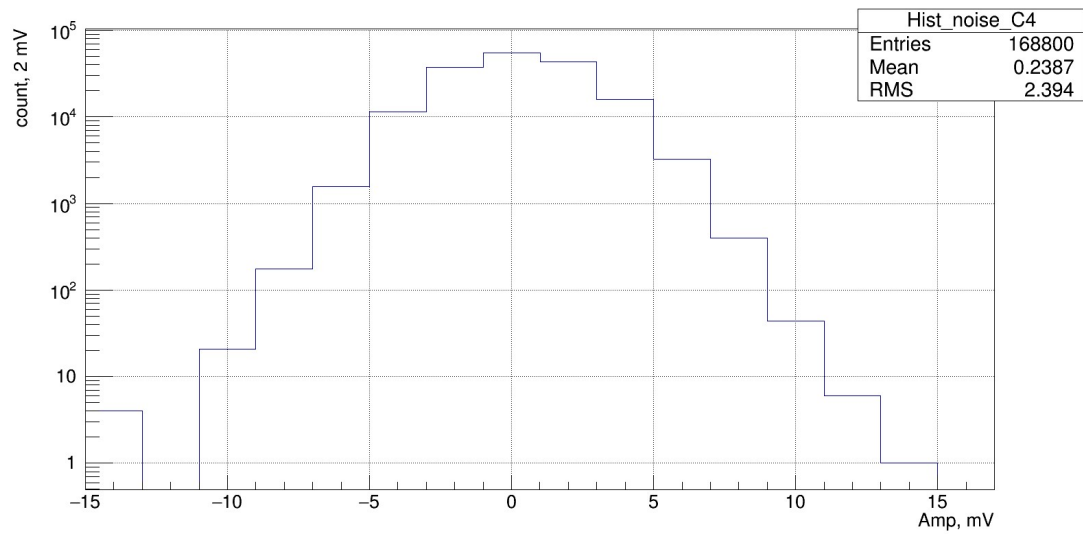
Fig. 4.2.2. Noise of 10 gaps MRPC.

4.3 Amplitude spectra

The amplitude spectra of the detectors with a gap of 175µm and 10 gaps MRPC are shown in fig. 4.2.3, 4.2.4. Obtained amplitude spectra are consistent with the theoretical expectations. We can control the presence of streamers by these histograms.
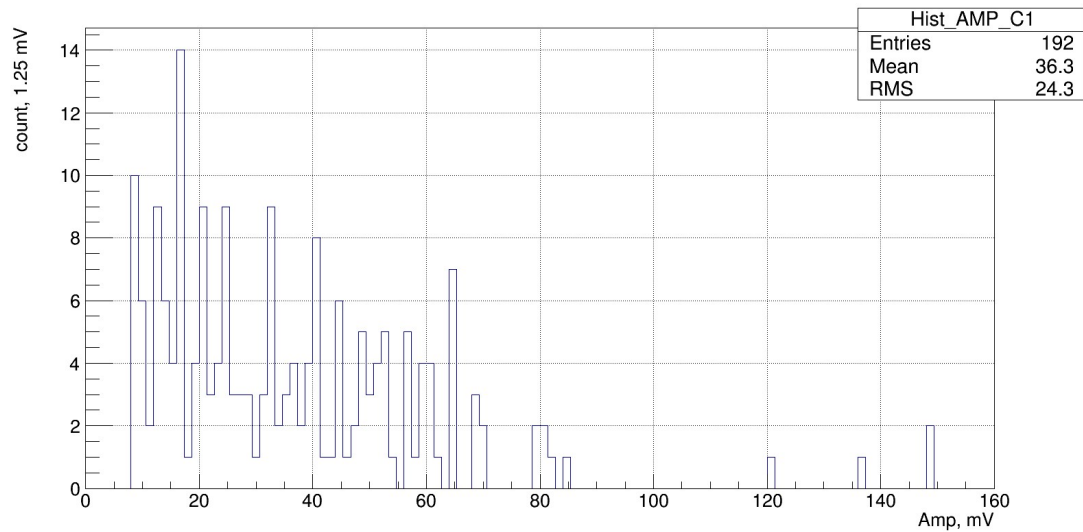
Fig. 4.2.1. The amplitude spectrum of the detector with a gap of 175µm.
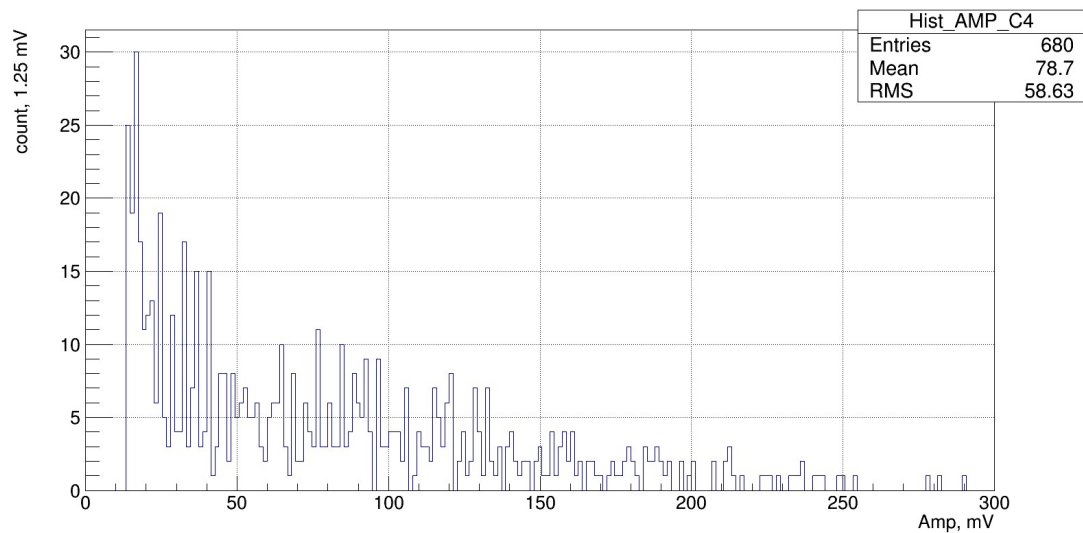
Fig. 4.2.2. The amplitude spectrum of 10 gaps MRPC.

4.3 Time distributions

There are time distribution histogram (fig. 4.3.1, 4.3.2).
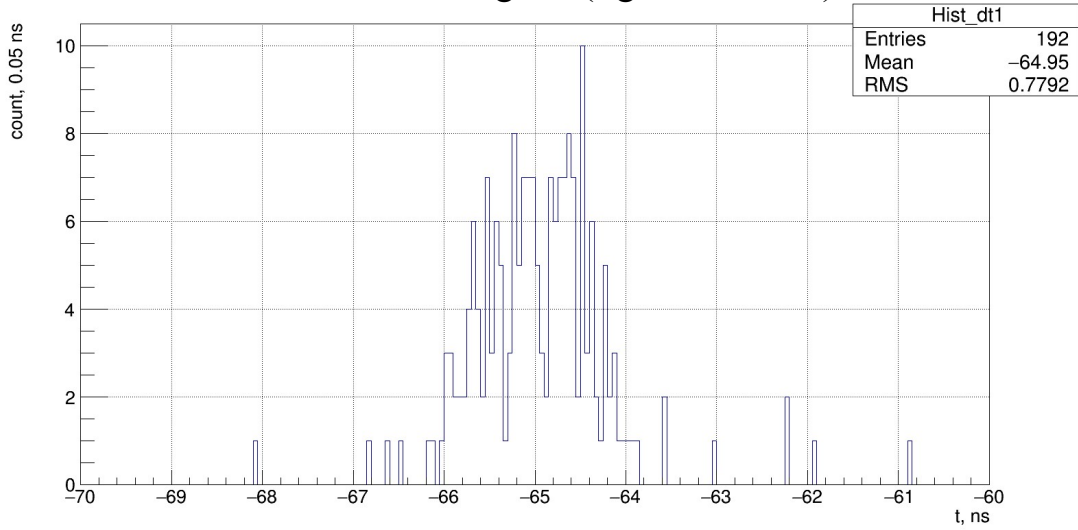
Fig. 4.3.1. The time distribution of the detector with a gap of 175µm.
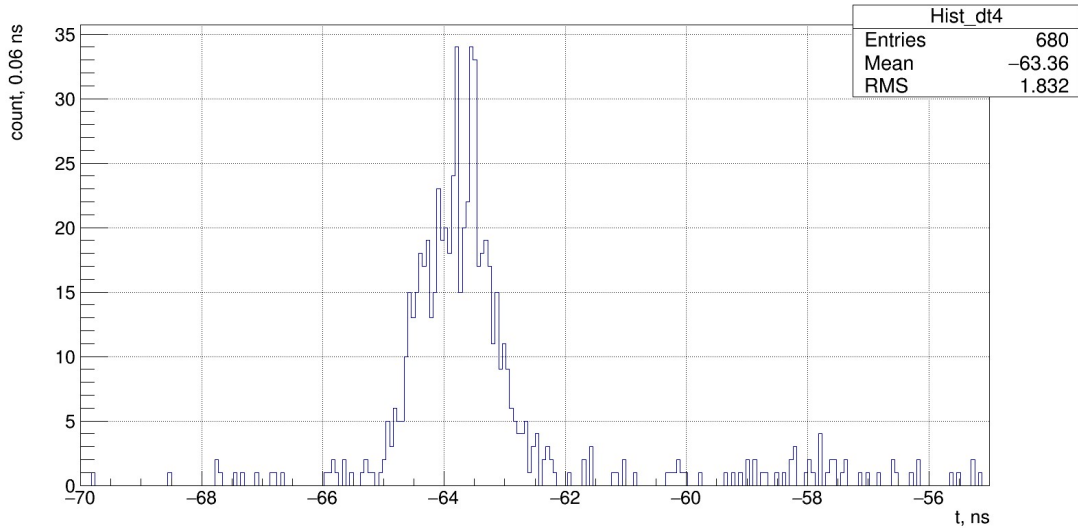
Fig. 4.3.2. The time distribution of 10 gaps MRPC.
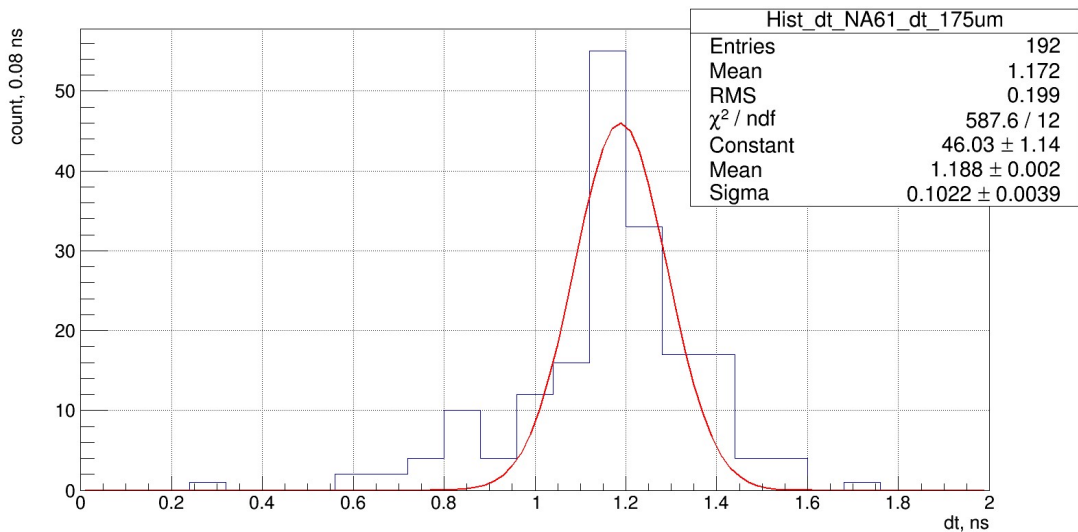
Fig. 4.3.3. The distribution of the time difference.

The time resolution of the tested detector is determined from the difference of times between the two detectors. An additional detector is not perfect and has time resolution. Therefore, the time resolution of a difference of times, there is nothing like the amount of time resolutions additional testing of the detector. And to find the time resolution of the tested detector we need to:

$$\sigma_{test} = \sqrt{\sigma_{com}^2 - \sigma_{add}^2} = \sqrt{102^2 - 60^2} \approx 82 \ ps$$

Thus, the thin-gap RPC have time resolution of 82 ps.

4.5 Efficiency calculating

On the basis of MRPC full efficiency, we have defined the efficiency of single gap as the ratio of the coincidence signals from both detectors to useful 10 gaps MRPC signals. Therefore,

$$p = \frac{192}{680} \approx 0.282$$

Consequently, ineffectiveness of one gap is

$$q = 1 - p = 0.718$$

Bernoulli's theorem states that the probability of p event for n independent trials can be found k times as

$$V = C_n^k p^k q^{n-k}$$

To achieve full efficiency it is necessary to fulfill condition:

$$V_m = \sum_{i=0}^{m} V_i = 0.99$$

Efficiency dependence on the number of gaps is shown in tab. 1 and fig. 4.5.

Gaps quantity	Efficiency
1	0,2823529412
2	0,4849826990
3	0,6303993487
4	0,7347571796
5	0,8096492701
6	0,8633953585
7	0,9019660808
8	0,9296462462
9	0,9495108355
10	0,9637665996
11	0,9739972068
12	0,9813391719
13	0,9866081116
14	0,9903893507

Table 1. Efficiency dependence on number of gaps.
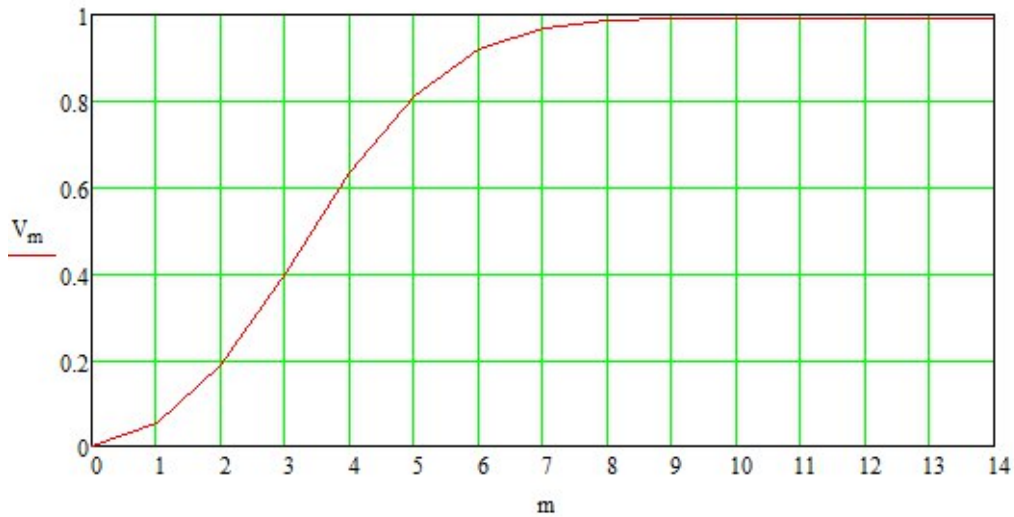
Fig. 4.5. Efficiency dependence on the number of gaps.

According to calculation we will achieve full efficiency at using 14 gaseous gaps. Also we can estimate time resolution from this formula:

$$\frac{\sigma_{com}}{\sqrt{m}} = 2.138 * 10^{-1}$$

Therefore, time resolution of 14 thin-gaps detector is 21 ps.

5 Conclusions

In this study the main problem is definition some properties and characteristics of the thin-gap resistive plate chamber. Test setup has collected data on cosmic rays. A key problem was determine the effectiveness of one gap with 175 μm width at fixed high voltage amplitude. According to the research results, it was calculated that the effectiveness of such gap is approximately 28% and time resolution is 102 ps. Thus, it will be sufficiency to use 14 gaps for achieve full efficiency and time resolution of 21 ps.

References

1. Multi-Purpose Detector (MPD)
http://nica.jinr.ru/projects/mpd.php

2. V. Babkin, *Triple-stack multigap resistive plate chamber with strip readout*, Nuclear Instruments and Methods in Physics Research Section A: Accelerators, Spectrometers, Detectors and Associated Equipment
Volume 824, 11 July 2016, Pages 490–492.

3. Werner Riegler, *Detector physics and simulation of resistive plate chambers*, Nuclear Instruments and Methods in Physics Research Section A: Accelerators, Spectrometers, Detectors and Associated Equipment
Volume 500, Issues 1–3, 11 March 2003, Pages 144–162.

4. V.A. Babkin, *Development of the MRPC for the TOF system of the MultiPurpose Detector*, JINR, Dubna(2016).

5. V.A. Babkin, *MPD NICA Technical Design Report of the Time of Flight System (TOF)*, TOF/MPD Collaboration JINR, Dubna(2015), Rev. 1.03.

6. Resistive Plate Chambers.
http://cms.web.cern.ch/news/resistive-plate-chambers